Reactions of Molybdenum and Tungsten Phosphenium Complexes with Sulfur and Selenium

Hans-Ulrich Reisacher, William F. McNamara, Eileen N. Duesler, and Robert T. Paine*

Department of Chemistry, University of New Mexico, Albuquerque, New Mexico 87131

Received July 8, 1996[⊗]

The reactions of the phosphane $[(Me_3Si)_2N](Ph)PCl$ with $NaCpMo(CO)_3$ and $NaCpW(CO)_3$ give the respective metallophosphenium complexes $Cp(CO)_2M\{P(Ph)[N(SiMe_3)_2]\}$ (M = Mo (**4a**), W (**4b**)). The subsequent reactions of **4a**,**b** with S and Se produce unexpectedly different products: $Cp(CO)_2(S)M\{P(Ph)[N(SiMe_3)_2]\}$ (M = Mo (**7a**)); $Cp(CO)_2\overline{MSP}(Ph)[N(SiMe_3)_2]$ (M = W (**7b**)); $Cp(CO)_2\overline{MSeP}(Ph)[N(SiMe_3)_2]$ (M = Mo (**8a**), W (**8b**)). The compounds have been fully characterized by elemental analyses and spectroscopic data, and the molecular structures of **4a**, **7a**,**b**, and **8a** have been determined by single-crystal X-ray diffraction techniques. The molecular structure of **7a** displays a long, terminal Mo−S bond, while **7b** and **8a** contain $\overline{M-E-P}$ three-membered rings.

Introduction

The reactions of monochlorophosphanes, (X)(Y)PCl, with $NaCpM(CO)_3$ (M = Cr, Mo, W) produce, via salt elimination, the neutral metallophosphane complexes $CpM(CO)_3[P(X)(Y)]$ (**1**) (Scheme 1).[1−4] The phosphorus atom in **1** is pyramidal, and the M−P bond is formally pure σ in character. Due to the Lewis basicity of the phosphane center and the lability of the CO ligands, examples of **1** tend to decarbonylate, forming neutral metallophosphenium complexes **2**.[1−4] Despite this fact, As and Sb analogs of **1** have been identified in matrix isolation infrared spectroscopic studies,[5] and the molecular structures of $CpM(CO)_3[P{=}C(SiMe_3)_2]$[2f] (M = Mo, W) and $CpMo(CO)_3\{P(Cl)[(^tBu_3C_6H_2O)]\}$[3e] have been determined by single-crystal X-ray diffraction techniques. Structural determinations for examples of **2** are more abundant, and these compounds feature a trigonal planar phosphorus atom environment and a short, formal M=P multiple bond.[1−4]

Scheme 1

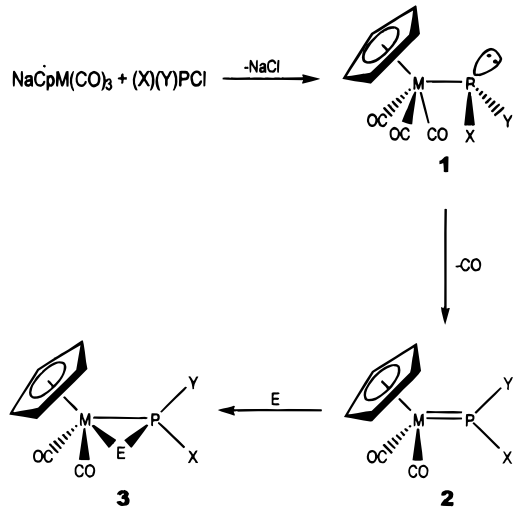

The chemistry of **1** and **2** has been of interest in several groups.[1−4] Much of the reactivity of **1** derives from the nucleophilicity of the uncommitted phosphorus lone pair, and additions of $H_3B{\cdot}THF$, $Ni(CO)_4$, and CH_3I to $CpW(CO)_2(Me_3P)(PPh_2)$, for example, result in formation of adducts $CpW(CO)_2(Me_3P)[P(A)(Ph)_2]$ (A = H_3B, $(CO)_3Ni$, and CH_3^+).[2d] Oxidations with S_8 and Br_2 also occur at the electron-rich PPh_2 center.

The nucleophilic reactivity of the planar phosphorus atom of **2** should be diminished since the phosphorus lone pair present in **1** is now involved in M=P multiple

[⊗] Abstract published in *Advance ACS Abstracts,* January 1, 1997.

(1) (a) Cowley, A. H.; Kemp, R. A. *Chem. Rev.* **1985**, *85*, 367. (b) Cowley, A. H.; Norman, N. C.; Quashie, S. *J. Am. Chem. Soc.* **1984**, *106*, 5007. (c) Arif, A. M.; Cowley, A. H.; Quashie, S. *J. Chem. Soc., Chem. Commun.* **1986**, 1437. (d) Cowley, A. H.; Giolando, D. N.; Nunn, C. M.; Pakulski, M.; Westmoreland, D; Norman, N. C. *J. Chem. Soc., Dalton Trans.* **1988**, 2127. (e) Arif, A. M.; Cowley, A. H.; Nunn, C. M.; Quashie, S.; Norman, N. C.; Orpen, A. G. *Organometallics* **1989**, *8*, 1878.

(2) (a) Gross, E.; Jörg, K.; Fiederling, K.; Göttlein, A.; Malisch, W.; Boese, R. *Angew. Chem., Int. Ed. Engl.* **1984**, *23*, 738. (b) Jörg, K.; Malisch, W.; Reich, W.; Meyer, A.; Schubert, U. *Angew. Chem., Int. Ed. Engl.* **1986**, *25*, 92. (c) Malisch, W.; Jörg, K.; Hofmockel, U.; Schmeusser, M.; Schemm, R.; Sheldrick, W. S. *Phosphorus Sulfur* **1987**, *30*, 205. (d) Malisch, W.; Jörg, K.; Gross, E.; Schmeusser, M.; Meyer, A. *Phosphorus Sulfur* **1986**, *26*, 25. (e) Maisch, R.; Ott, E.; Buchner, W.; Malisch, W.; Sheldrick, W. S.; McFarlane, W. *J. Organomet. Chem.* **1985**, *286*, C31. (f) Gudat, D.; Niecke, E.; Malisch, W.; Hofmockel, U.; Quashie, S.; Cowley, A.; Arif, A. M.; Krebs, B.; Dartmann, M. *J. Chem. Soc., Chem. Commun.* **1985**, 1687. (g) Malisch, W.; Maisch, R.; Colquhoun, I. J.; McFarlane, W. *J. Organomet. Chem.* **1981**, *220*, C1.

(3) (a) Lang, H.; Leise, M.; Zsolnai, L. *Polyhedron* **1992**, *11*, 1281. (b) Lang, H.; Leise, M.; Imhof, W.; *Z. Naturforsch.* **1991**, *46b*, 1650. (c) Lang, H.; Leise, M.; Zsolnai, L.; Fritz, M. *J. Organomet. Chem.* **1990**, *395*, C30. (d) Lang, H.; Leise, M.; Zsolnai, L. *J. Organomet. Chem.* **1990**, *389*, 325. (e) Leise, M.; Zsolnai, L.; Lang, H. *Polyhedron* **1993**, *12*, 1257. (f) Lang, H.; Leise, M.; Zsolnai, L. *Organometallics* **1993**, *12*, 2393.

(4) (a) Light, R. W.; Paine, R. T. *J. Am. Chem. Soc.* **1978**, *100*, 2230. (b) Hutchins, L. D.; Paine, R. T.; Campana, C. F. *J. Am. Chem. Soc.* **1980**, *102*, 4521. (c) Hutchins, L. D.; Reisacher, H.-U.; Wood, G. L.; Duesler, E. N.; Paine, R. T. *J. Organomet. Chem.* **1987**, *335*, 229. (d) Dubois, D. A.; Duesler, E. N.; Paine, R. T. *Organometallics* **1983**, *2*, 1903. (e) Hutchins, L. D.; Duesler, E. N.; Paine, R. T. *Organometallics* **1984**, *3*, 399. (f) McNamara, W. F.; Duesler, E. N.; Paine, R. T.; Ortiz, J. V.; Kölle, P.; Nöth, H. *Organometallics* **1986**, *5*, 380. (g) Paine, R. T.; McNamara, W. F.; Janik, J. F.; Duesler, E. N. *Phosphorus Sulfur* **1987**, *30*, 241. (h) Reisacher, H.-U.; Duesler, E. N.; Paine, R. T. *Chem. Ber.* **1996**, *129*, 279. (i) Hutchins, L. D. Ph.D. Thesis, University of New Mexico, 1983.

(5) Mahmoud, K. A.; Rest, A. J.; Luksza, M.; Jörg, K.; Malisch, W. *Organometallics* **1984**, *3*, 501.

S0276-7333(96)00549-3 CCC: $14.00

bonding. Experimentally, Malisch reports that $CpM(CO)_2[POCMe_2CMe_2O]$ (M = Cr, Mo, W)[2d] and $CpMo[P(NMe_2)_2]$[2a] react with S_8 to give thio-bridged species **3a** (E = S). Similarly, reaction of CH_2N_2 with the former compound produces a [2+1] cycloaddition species **3b** (E = CH_2), and addition of $Fe_2(CO)_9$ results in **3c** (E = $Fe(CO)_4$). Another example of **2**, $CpW(CO)_2[P(^tBu)_2]$, reacts with S_8, Se, CH_2N_2, $(MeP)_5$, Me_2P, $Fe_2(CO)_9$, and $Ru_3(CO)_{10}$, each forming [2+1] cycloaddition products **3**.[2c] In addition, Lang[3b,f] describes reactions on bifunctional σ^3,λ^4-phosphanediyl phosphenium complexes, $CpM(CO)_2[P(R)C{\equiv}CR]$, $CpM(CO)_2[P(R)C(H){=}C(H)R]$, and $CpM(CO)_2[P(R)CH_2C{\equiv}CH]$, which undergo [2+1] cycloadditions with CH_2N_2, $Fe(CO)_5$, PhN_3, and $(2,4,6\text{-}Me_3C_6H_2)N_3$. Finally, by using different synthetic strategies, Nakazawa[6] outlines reactions of a cationic metallophosphenium species $CpFe(CO)(R)[PN(Me)CH_2CH_2N(Me)]$, which readily undergoes migratory insertion and base addition to produce, for example, $\{CpFe(CO)(PPh_3)[PN(Me)CH_2CH_2N(Me)(R)]\}BF_4$.

These observations clearly show that the reactivity of **1** and **2** differ, but the phosphorus atom seems to retain some nucleophilic activity. In fact, we have observed that $H_3B{\cdot}THF$ adds across the M=P double bond in $CpMo(CO)_2\{P(Ph)[N(Me_3Si)_2]\}$ (**4a**) giving **5**.[4f]

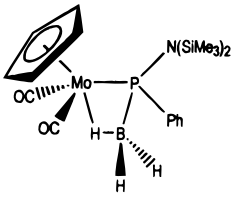

5

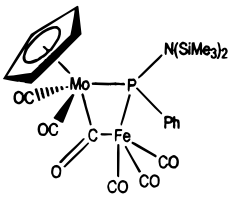

6

In addition, we find that **4a** reacts with $Fe_2(CO)_9$ to give **6**,[4h] which does not feature a simple three-membered ring core as in **3** but instead displays a bridging CO interaction between the Mo and Fe centers. In the present report, the oxidation reactions of **4a** and $CpW(CO)_2\{P(Ph)[N(SiMe_3)_2]\}$ (**4b**) with S_8 and Se are described along with spectroscopic and single-crystal X-ray diffraction studies.

Results and Discussion

The 1:1 combinations of $[(Me_3Si)_2N](Ph)PCl$ with $NaCpMo(CO)_3$ and $NaCpW(CO)_3$ in THF solution produce metallophosphenium complexes $Cp(CO)_2Mo\{P(Ph)[N(SiMe_3)_2]\}$ (**4a**) and $Cp(CO)_2W\{P(Ph)[N(SiMe_3)_2]\}$ (**4b**) in high yields as crystalline purple solids that are moisture and air sensitive. This chemistry is illustrated in Scheme 2. It is likely that the respective metallophosphane complexes $Cp(CO)_3M\{P(Ph)[N(SiMe_3)_2]\}$(Mo (**9a**); W (**9b**)) form at low temperature as indicated by the rapid color change in the reaction solution without noticeable formation of CO. Upon standing of the solution at −78 °C, CO is slowly released and approximately 30% of the expected CO is recovered after 6 h by using a Toepler pump. The overall rate of CO loss is enhanced by continuous removal of the CO and/or by running the reaction at 23 °C or at THF reflux. With reflux, 90−100% of the expected CO is released in about 6 h. No effort was made to isolate or characterize the intermediate species **9**.

Scheme 2

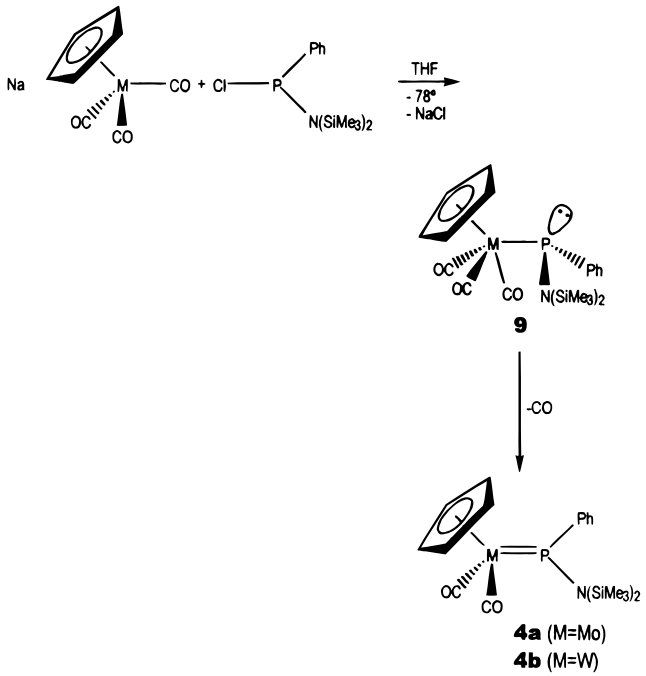

Compounds **4a**,**b** each show a parent ion envelope (*m/e* 433−423, **4a**, and *m/e* 576−571, **4b**) in electron impact mass spectra as well as an intense fragment ion envelope [M − $2CO^+$]. The infrared spectra of the compounds show two strong bands in the terminal carbonyl stretching region: **4a**, 1948 and 1876 cm^{-1}; **4b**, 1941 and 1869 cm^{-1}. These data are consistent with the presence of two terminal CO groups, and they compare favorably with values of 1954 and 1876 cm^{-1} reported previously for $Cp(CO)_2MoP(NMe_2)_2$.[4c] The $^{31}P\{^1H\}$ NMR spectra each show a single, low-field resonance typical of metallophosphenium complexes: **4a**, δ 316; **4b**, δ 267.[4] The resonance for **4b** also shows satellites due to tungsten−phosphorus coupling, and the large value, $^1J_{PW}$ = 702 Hz, is consistent with the anticipated strong M=P σ/π overlap involving a planar, formally sp^2-hybridized phosphenium ion center. The $^{13}C\{^1H\}$ and ^1H NMR spectra show resonances that are unambiguously assigned to the $N(SiMe_3)_2$, Cp, and phenyl groups.

The molecular structure of **4a** was determined by single crystal X-ray diffraction analysis,[7] and a view of the molecule is shown in Figure 1. Selected bond distances and angles are summarized in Table 2. The molecule has C_1 symmetry with the molybdenum atom having a three-legged piano stool pseudo-octahedral geometry. The average Mo−CO and MoC≡O distances, 1.949(3) and 1.151(5) Å, are identical to the values displayed by $CpMo(CO)_2[POCH_2CH_2NCMe_3]$[4e] (**10**),

(6) Nakazawa, H.; Yamaguchi, Y.; Mizuta, T.; Ichimura, S.; Miyoshi, K. *Organometallics* **1995**, *14*, 4635.

(7) The molecular structure of **4b** was also determined; however, disorder in the phenyl ring precluded full anisotropic refinement. The crystallographic data include: monoclinic, space group *Cc* (No. 9), a = 12.475(1) Å, b = 11.319(3) Å, c = 16.777(5) Å, $\alpha = \gamma = 90°$, β = 102.92(2)°, V = 2309.0(12) $Å^3$, Z = 2, D_{calcd} = 1.39 g cm^{-3}. The molecular structure was essentially identical to that observed for **4a** with W−P = 2.252(6) Å and P−N = 1.68(2) Å.

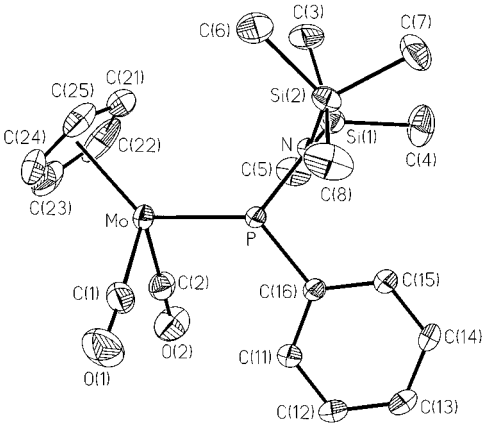

Figure 1. Molecular geometry and atom-labeling scheme for $Cp(CO)_2Mo\{P(Ph)[N(SiMe_3)_2]\}$ (**4a**) with H atoms omitted. Thermal ellipsoids are represented at the 25% probability level.

$CpMo(CO)_2[\overline{PN(Me)CH_2CH_2NMe}]$[4a] (**11**), and $CpMo(CO)_2[\overline{PN(bz)CH_2CH_2N(bz)}]$[4c] (**12**). The C(1)−Mo−C(2) bond angle, 81.7(1)°, on the other hand, is somewhat smaller than the angles observed in **10** (86.1(2)°), **11** (85.3(3)°), and **12** (85.2(3)°), which contain cyclic phosphenium ion fragments. The Mo, P, N, and C(16) atoms form a plane[8] that is approximately perpendicular to the $Mo(CO)_2$ plane (interplanar angle 98.6°), and the sums of angles about the P and N atoms are 359.2 and 359.3°, respectively. The P, N, Si(1), and Si(2) atoms also comprise a plane,[8] and it makes an angle of 91.2° with the MoPNC(16) plane. The Mo−P distance of 2.248(1) Å is short compared with the typical range of P→Mo dative bond lengths (2.42−2.53 Å)[9] found in metal phosphane complexes,[9] and this bond shortening has been previously offered[1−4] in support of Mo=P multiple bonding. It is interesting, however, that the bond shortening in **4a** is not as large as found in **10** (2.207(1) Å), **11** (2.213(1) Å), and **12** (2.212(2) Å), which suggests that the $P(Ph)[N(SiMe_3)_2]^+$ fragment may be a weaker π-acid. This is consistent with the changes in substituent groups on the fragment relative to $P(NR_2)_2^+$ and $P(OR)(NR_2)^+$ species. The P−N distance of 1.698(2) Å is also significantly longer than the P−N bond lengths in **10** (1.660(3) Å), **11** (1.645(5) Å), and **12** (1.655 Å (avg)). This is consistent with the presence of competitive π overlap between the N and Si atoms that would be expected to reduce the N−P π bond interaction. The P−N distance in **4a** is, in fact, closer to the value found in the phosphane $(H_3Si)_2NPF_2$,[10] 1.680(4) Å. The Si−N distance in **4a**, 1.764 Å (avg), is comparable with the Si−N distance in $(H_3Si)_2NPF_2$, 1.755(4) Å.

Subsequent combinations of **4a**,**b** with an equimolar amount of sulfur in methylcyclohexane or benzene solution at −78 °C produce no reactions; however, upon warming of the solution to 0 °C and then room temperature, the purple color of **4** is discharged and replaced by a yellow-orange color. Analysis of the raw reaction mixtures by infrared and ^{31}P NMR spectroscopy shows a complete disappearance of **4** from the reaction mixture and the appearance of two new ν_{CO} frequencies and a single ^{31}P NMR resonance. The products **7a**,**b** are isolated in high yield and recrystallized as orange crystalline solids. The chemistry is summarized in eq 1.

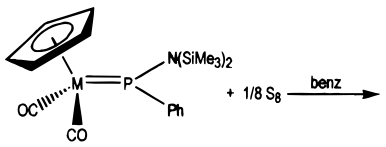

4

$Cp(CO)_2M(S)P(Ph)[N(SiMe_3)_2]$ (1)

7

The mass spectra for compounds **7a**,**b** display a parent ion envelope as well as fragment ion envelopes corresponding to $[M - CO^+]$ and $[M - 2CO^+]$. In each case, the $[M - 2CO^+]$ envelope is considerably more intense than the $[M - CO^+]$ envelope. The infrared spectra for the compounds show two bands in the CO stretch region: **7a**, 1960 and 1886 cm^{-1}, and **7b**, 1952 and 1873 cm^{-1} (cyclohexane solution). These are shifted only slightly up-frequency from the respective starting materials **4a**,**b**. Each compound shows a single ^{31}P NMR resonance centered at δ 73 and 33.9, respectively. The latter resonance shows satellite doublet splitting $^1J_{PW} = 268.6$ Hz. This is significantly reduced from the value in **4b** and suggests that the phosphorus atom is in a pyramidal environment. The ^{13}C and ^1H NMR data show resonances that are assigned to the Me_3Si, Cp, and Ph groups, and they are shifted only slightly from those in the starting materials. It is interesting to note that both compounds display two $^{13}C\{^1H\}$ resonances for the $(CH_3)_3Si$ groups indicating that they are in inequivalent environments. The ^1H NMR spectrum for **7a** displays two singlets of equal intensity for the $N(SiMe_3)_2$, and their resonance positions are nearly 1 ppm downfield of the singlet observed for **7b**. These are the only spectroscopic data that suggest that **7a**,**b** may have different structures.

The molecular structure of **7a** was determined by X-ray diffraction techniques, and a view of the molecule is shown in Figure 2. Selected bond distances and angles are presented in Table 2. Somewhat surprisingly, **7a** *does not* display either of the expected structures, **7′** or **7″**, shown here. Instead, the compound has

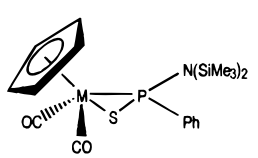

7'

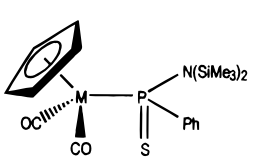

7"

a four-legged piano stool structure in which the Mo atom is seven coordinate and bonded to an η^5-C_5H_5 ring, two terminal CO groups, the phosphorus atom of the phosphenium ion ligand, and a *terminal* sulfur atom. The molecule has C_1 symmetry, and the CO groups are *cis*

(8) The least-squares plane involving the MoPN and C(16) atoms calculated for **4a** is described by $10.6589x - 0.9025y + 5.2963z = 0.6029$. The deviations from the plane are as follows: Mo, 0.023 Å; P, −0.071 Å; N, 0.024 Å, C(16), 0.023 Å. The plane involving PN Si(1) and Si(2) is described by $3.8812x + 9.6735y - 8.0053z = 7.3523$. The deviations from the plane are as follows: P, −0.0214 Å; N, 0.0649 Å; Si(1), −0.0218 Å, and Si(2), −0.0217 Å.

(9) Corbridge, D. E. C. *The Structural Chemistry of Phosphorus*; Elsevier: Amsterdam, 1974.

(10) Laurenson, G. S.; Rankin, D. W. H. *J. Chem. Soc., Dalton Trans.* **1981**, 425.

Table 1. Crystallographic Data for $Cp(CO)_2Mo\{P(Ph)[N(SiMe_3)_2]\}$ (4a), $Cp(CO)_2Mo(S)\{P(Ph)[N(SiMe_3)_2]\}$ (7a), $Cp(CO)_2WSP(Ph)[N(SiMe_3)_2]$ (7b), and $Cp(CO)_2MoSeP(Ph)[N(SiMe_3)_2]$ (8a)

	4a	7a	7b	8a
mol formula	$C_{19}H_{28}NO_2Si_2PMo$	$C_{19}H_{28}NO_2Si_2PSMo$	$C_{19}H_{28}NO_2Si_2PSW$	$C_{19}H_{28}NO_2Si_2PSeMo$
fw	485.5	517.6	605.5	564.52
cryst syst	monoclinic	triclinic	monoclinic	tetragonal
space group	*Cc*	$P\bar{1}$ (No. 2)	$P2_1/n$	$P4_1$ (No. 76)
a, Å	12.527(2)	9.673(2)	11.396(1)	10.228(1)
b, Å	11.328(2)	11.328(2)	17.245(3)	10.228(1)
c, Å	16.789(2)	11.579(2)	12.309(2)	23.191(3)
α, Å	90	87.29(2)	90	90
β, Å	102.95(1)	77.82(1)	91.49(1)	90
γ, Å	90	82.74(2)	90	90
V, Å^3	2321.9(6)	1230.0(4)	2418.2(5)	2426.0(6)
Z	4	2	4	4
μ, cm^{-1}	7.32	7.74	53.1	23.2
D_{calcd}, g cm^{-3}	1.39	1.397	1.66	1.55
F(000)	1000	532	1192	1136
cryst dimens, mm	0.25 × 0.41 × 0.46	0.23 × 0.23 × 0.08	0.14 × 0.25 × 0.39	0.23 × 0.41 × 0.69
reciprocal space	$\pm h,k,\bar{l}$ and $\pm h,\bar{k},l$	$\pm h,\pm k,\pm l$	$\pm h,+k,+l$	$\pm h,k,l$
scan type	$\theta-2\theta$	ω	$\theta-2\theta$	ω
$2\theta_{max}$, deg	60	50	55	55
$T_{min/max}$	0.498/0.521	0.802/0.877	0.392/1.00	0.235/0.259
no. of reflcns measd	7632	7593	12,288	13,129
unique reflcns	6732	4344	5544	5582
obsd reflcns	5924, $F > 5\sigma(F)$	3237, $F > 4\sigma(F)$	4573, $F > 3\sigma(F)$	5262, $F > 3\sigma(F)$
params refined	233	274	244	108
R^a/R_w	0.0267/0.0273	0.0457/0.0359	0.0644/0.0508	0.0753/0.084

[a] $R = \Sigma(||F_o| - |F_c||)/\Sigma|F_o|$; $R_w = [\Sigma w(|F_o| - |F_c|)^2/\Sigma w|F_o|^2]^{1/2}$.

Table 2. Structural Parameters for $Cp(CO)_2Mo\{P(Ph)[N(SiMe_3)_2]\}$ (4a), $Cp(CO)_2Mo(S)\{P(Ph)[N(SiMe_3)_2]\}$ (7a), $Cp(CO)_2WSP(Ph)[N(SiMe_3)_2]$ (7b), and $Cp(CO)_2MoSeP(Ph)[N(SiMe_3)_2]$ (8a)

(a) Bond Lengths (Å)

	4a		7a		7b		8a	
M−P	Mo−P	2.248(1)	Mo−P	2.519(1)	W−P	2.411(2)	Mo−P	2.411(1)
M−CO	Mo−C(1)	1.948(3)	Mo−C(1)	1.948(5)	W−C(1)	1.939(9)	Mo−C(1)	1.957(4)
	Mo−C(2)	1.951(3)	Mo−C(2)	1.952(6)	W−C(2)	1.950(9)	Mo−C(2)	1.959(4)
C≡O	C(1)−O(1)	1.150(5)	C(1)−O(1)	1.145(6)	C(1)−O(1)	1.155(11)	C(1)−O(1)	1.148(6)
	C(2)−O(2)	1.153(4)	C(2)−O(2)	1.145(7)	C(2)−O(2)	1.162(11)	C(2)−O(2)	1.150(6)
P−C	P−C(16)	1.819(2)	P−C(16)	1.835(4)	P−C(8)	1.820(6)	P−C(3)	1.826(4)
P−N	P−N	1.698(2)	P−N	1.695(4)	P−N	1.680(6)	P−N	1.682(3)
Si−N	Si(1)−N	1.763(2)	Si(1)−N	1.774(3)	Si(1)−N	1.784(6)	Si(1)−N	1.779(3)
	Si(2)−N	1.766(2)	Si(2)−N	1.774(3)	Si(2)−N	1.781(6)	Si(2)−N	1.783(4)
P−S					P−S	2.023(2)		
P−Se							P−Se	2.168(1)
M−S			Mo−S	2.509(1)	W−S	2.538(2)		
M−Se							Mo−Se	2.671(1)

(b) Bond Angles (deg)

4a		7a		7b		8a	
C(1)−Mo−C(2)	81.7(1)	C(1)−Mo−C(2)	75.1(2)	C(1)−W−C(2)	77.0(4)	C(1)−Mo−C(2)	77.3(2)
Mo−P−C(16)	128.7(1)	Mo−P−C(16)	118.4(2)	W−P−C(8)	122.9(2)	Mo−P−C(3)	122.9(1)
Mo−P−N	127.3(1)	Mo−P−N	123.5(1)	W−P−N	126.9(2)	Mo−P−N	125.9(1)
N−P−C(16)	103.2(1)	N−P−C(16)	105.6(2)	N−P−C(8)	106.1(3)	N−P−C(3)	106.1(2)
		S−Mo−P	74.1(2)	S−P−C(8)	109.7(2)	Se−P−C(3)	107.7(1)
				W−P−S	69.2(1)	Mo−P−Se	71.1(1)
				W−S−P	71.1(6)	Mo−Se−P	58.7(1)
				S−W−P	48.2(1)	Se−Mo−P	50.2(1)

to each other. There is no evidence for a *trans* isomer in the solid state or in solution as determined by the ^{31}P NMR spectra at 23 °C.

The M−CO and C≡O bond lengths in **7a** are identical within experimental error to those found in **4a**. The C(1)−Mo−C(2) bond angle, 75.1(2)°, is slightly compressed from that in **4a**. The Mo−C bond distances involving the Cp ring are more asymmetric than in **4a**, Mo−C(21) (2.390(5) Å), Mo−C(22) (2.311(5) Å), Mo−C(23) (2.271(6) Å), Mo−C(24) (2.290(5) Å), and Mo−C(25) (2.385(6) Å), and the average value 2.329 Å is slightly shorter than the average M−C distance in **4a**, 2.348 Å. The C−C bond distances within the ring also vary (1.419(8)−1.370(10) Å, avg 1.394 Å); however, the size of the esd's make detailed comparisons of these distances undependable. Similar distortions in other CpMo(S) fragments have been noted,[11] and it has been suggested that these result from electronic perturbations within the fragment.[12] The phosphorus atom now

(11) Rakowski-DuBois, M.; DuBois, D. L.; Van Derveer, M. C.; Haltiwanger, R. C. *Inorg. Chem.* **1981**, *20*, 3064.

(12) Mingos, D. M. P.; Minshall, P. C.; Hursthouse, M. B.; Willoughby, S. D.; Malid, K. M. A. *J. Organomet. Chem.* **1979**, *181*, 169. Mingos, D. M. P. *Trans. Am. Crystallogr. Assoc.* **1980**, *16*, 17.

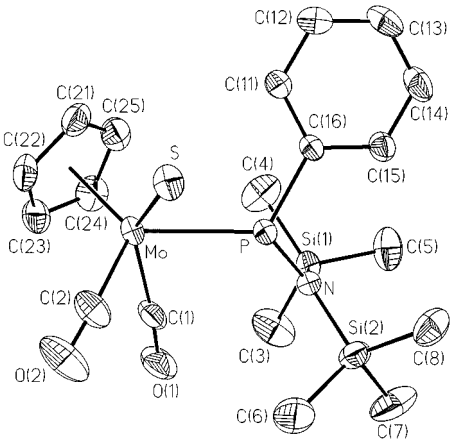

Figure 2. Molecular geometry and atom-labeling scheme for $Cp(CO)_2(S)Mo\{P(Ph)[N(SiMe_3)_2]\}$ (**7a**) with H atoms omitted. Thermal ellipsoids are represented at the 25% probability level.

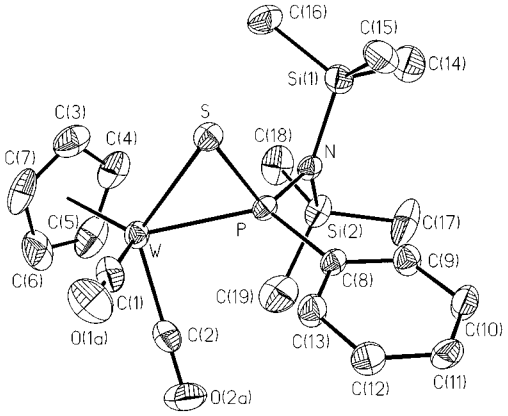

Figure 3. Molecular geometry and atom-labeling scheme for $Cp(CO)_2\overline{WSP}(Ph)[N(SiMe_3)_2]$ (**7b**) with H atoms omitted. Thermal ellipsoids are represented at the 25% probability level.

displays a pyramidal geometry with a sum of bond angles of 347.5°, and the Mo−P distance of 2.519(1) Å is substantially longer than in **4a**, which places it at the upper end of the range of Mo−P single bond distances. In fact, it is comparable to the value in the related compound *cis*-$CpMo(CO)_2(Br)(PPh_3)$, 2.538(2) Å.[13] The terminal Mo−S distance, 2.509(1) Å, is relatively long and certainly outside the typical range found for terminal Mo═S bonds (1.937−2.129 Å).[14] It is also longer than the Mo−S single bond distances in several M−S−M bridged conditions: $[(MeC_5H_4)MoS_2]_2$ (2.300(2) Å),[11] MoS_9^{2-} (2.359(1) Å),[15] $[(CS_4)_2MoS]^{2-}$ (2.35(3) Å).[16] This might suggest that **7a** has the sulfur-bridging structure depicted by **7′**; however, the P···S separation is 3.032 Å, which is well beyond the sum of covalent radii, 2.47 Å. Further, despite the bulky nature of the $(Me_3Si)_2N$ and Ph groups on the phosphorus atom, the arrangement of the four piano stool legs around the Mo atom is relatively symmetrical, as indicated by the following bond angles: P−Mo−S (74.1( )°), S−Mo−C(2) (79.3(2)°), C(2)−Mo−C(1) (76.1(2)°), and C(1)−Mo−P (79.0(2)°). Thus the Mo−S bond vector cannot be considered as displaced toward the P atom.

The P−N distance in **7a**, 1.695(4) Å, is unchanged from that in **4a**, and the P−C(16) distance, 1.835(4) Å, is only slightly elongated compared to the starting material. The N atom is still trigonal planar in **7a**, and the average N−Si bond length, 1.774 Å, is slightly longer than the average distance in **4a**, 1.764 Å.

In contrast, the molecular structure determination for **7b** reveals the structure type **7′** suggested by Malisch.[2] A view of the molecule is shown in Figure 3, and selected bond lengths and angles are given in Table 2. The W, S, and P atoms form a three-membered ring in which the W−P distance 2.411(2) Å is intermediate between the values found for **4a**, **4b**,[7] and **7a**. Further, the P−S distance 2.023(2) Å is within the expected single bond range[9] as opposed to the nonbonding condition found in **7a**, while the W−S distance 2.538(2) Å is longer than the Mo−S distance in **7a**. The W−CO, C≡O, P−N, and P−C(phenyl) bond distances and the C(1)−W−C(2) angle are comparable with the corresponding parameters in **7a**. Although **7b** can be classed as a four-legged piano stool, the geometry about the W atom is much more asymmetric than in **7a** as indicated by the following angles: P−W−S (48.2(1)°), S−W−C(2) (122.3(3)°), C(2)−W−C(1) (77.0(4)°), and C(1)−W−P (103.0(3)°). This asymmetry is imposed by the formation of the three-membered $\overline{W-S-P}$ ring.

The reactions of **4a**,**b** with equimolar amounts of selenium were examined in C_6H_6 solution at room temperature. In both cases, the purple color of the starting material solution is rapidly converted to a dark red color upon addition of the Se, and the products $Cp(CO)_2\overline{MoSeP}(Ph)[N(SiMe_3)_2]$ (**8a**) and $Cp(CO)_2\overline{WSeP}(Ph)[N(SiMe_3)_2]$ (**8b**) are isolated in high yield as red crystalline solids. The chemistry is summarized in eq 2.

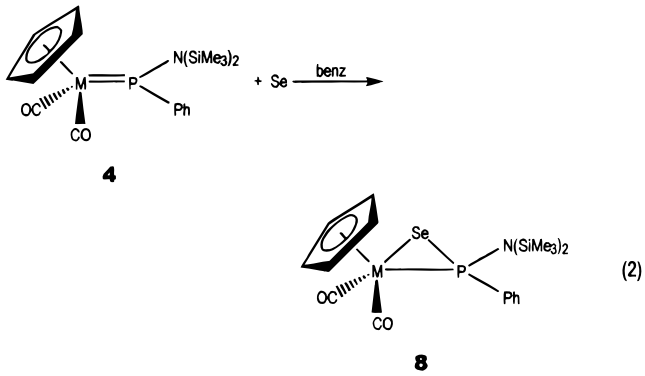

(2)

The mass spectra of both **8a**,**b** display a parent ion envelope as well as fragment ion envelopes corresponding to $[M - CO^+]$ and $[M - 2CO^+]$, and as with **7a**,**b**, the $\{M - 2CO^+]$ ion envelope is considerably more intense. Both compounds display two infrared bands in the CO stretch region: **8a**, 1959 and 1886 cm^{-1}, and **8b**, 1951 and 1875 cm^{-1} (cyclohexane solution). These data are identical to those found for **7a**,**7b**. The compounds show a single resonance in the ^{31}P NMR spectra, each split into doublets by P−Se coupling: **8a**, δ 85.9, $^1J_{PSe} = 497.8$ Hz; **8b**, δ 43.92, $^1J_{PSe} = 469.2$ Hz.

(13) Sim, G. A.; Sime, J. G.; Woodhouse, D. I.; Knox, G. R. *Acta Crystallogr.* **1979**, *35b*, 2403.
(14) Huneke, J. T.; Enemark, J. H. *Inorg. Chem.* **1978**, *17*, 3698.
(15) Simhon, E. D.; Baenziger, N. C.; Kanatzidis, M.; Draganjac, M.; Coucouvanis, D. *J. Am. Chem. Soc.* **1981**, *103*, 1218.
(16) Coucouvanis, D.; Draganjac, M. *J. Am. Chem. Soc.* **1982**, *104*, 6820.

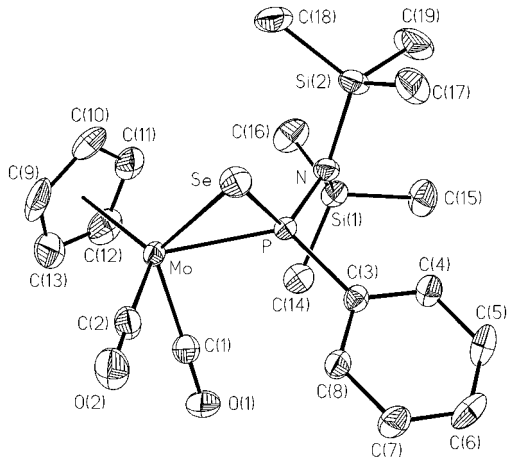

Figure 4. Molecular geometry and atom-labeling scheme for $Cp(CO)_2\overline{MoSeP}(Ph)[N(SiMe_3)_2]$ (**8a**) with H atoms omitted. Thermal ellipsoids are represented at the 25% probability level.

The latter also shows ^{184}W satellite coupling $^1J_{PW} = 290.2$ Hz. It is interesting that, like **7b**, the ^{31}P chemical shift for **8b** appears upfield of that for **8a**. The ^1H and ^{13}C NMR data are also consistent with the proposed formulation of the compound, and the $^{13}C\{^1H\}$ spectra reveal inequivalent $SiMe_3$ group environments.

The molecular structure of **8a** was determined and found clearly to have the structure type **7′**. A view of the molecule is shown in Figure 4, and bond lengths and angles are summarized in Table 2. The structure is virtually identical to that of **7b** except that the $\overline{MoSeP}$ three-membered ring is larger, as expected for substitution of S by Se: P−Se (2.168(1) Å) and Mo-Se (2.671(1) Å).

Summary

The results of this study demonstrate that the metallophosphenium complexes **4a**,**b** react with sulfur and selenium to produce, in each case, a single product in high yield. In three of the four combinations, metal−phosphorus−chalcogen three-membered ring structures of the general type illustrated by **7′** are formed. These are related to structures proposed earlier by Malisch and co-workers for related metallophosphenium species.[2a,d] However, combination of S_8 with **4a** produces an unusual and unexpected species **7a** that contains a terminal Mo−S single bond. Although the mechanism for these formal oxidation reactions is unknown and detailed MO analyses for **7** and **8** have not yet been attempted, some speculation on how the molecules form in two classes (**7a** vs **7b**, **8a** and **8b**) may be worthwhile based upon previous MO analyses for $Cp(CO)_2M[P(NR_2)_2]$[4b,i] and **5**.[4f,17] These calculations reveal that the metal−phosphorus bond in examples of **2** with $X = Y = NR_2$ can be considered to involve P atom lone pair donation from the planar phosphenium ion fragment $P(X)(Y)^+$ into an empty LUMO (d_{z^2}) on the $CpMo(CO)^{2-}$ fragment. This σ bond component is supplemented by π back-donation from an occupied metal d orbital (d_{xz}) on the $CpMo(CO)_2^-$ fragment into a vacant out-of-plane π^* symmetry MO distributed over the P atom and two N atoms of $P(X)(Y)^+$. In **4a**,**b**, since neither the Ph group nor the $N(SiMe_3)_2$ group will be as efficient at out-of-plane p orbital overlap compared to NR_2, the π back-donation from the metal will occur into an orbital more localized on the P atom. It is reasonable to assume that the HOMO in **4a**,**b** will be the π symmetry M→P MO, whose electron density will be largely localized on the P atom, or it will be the remaining occupied d orbital (d_{yz}) that is nonbonding with respect to the M−P(X)(Y) unit. These orbitals are probably very similar in energy, and the precise orbital composition of the HOMO will depend upon the electronic character of the substituents on the P atom and the specific metal atom and its substituents.

The electrons in the HOMO orbital of **4a**,**b** will be the focus of approaching electrophiles such as Lewis acids and oxidants. In the case of BH_3 attack on **4a** which produced **5**,[4f] it was suggested that the π-symmetry Mo→P HOMO donates electron density into the empty p orbital on the BH_3 fragment, forming a B−P σ bond. In addition, this is supplemented by interaction of the LUMO of **4** (the antibonding component of the Mo→P π bond) with electron density from one of the degenerate HOMO orbitals (B−H bonds) on the BH_3 fragment. This results in the B−H−Mo bridge bond that is largely polarized toward the metal. A similar picture may be utilized to rationalize the structure of **6** containing the CO group bridging the $Cp(CO)_2Mo$ fragment and the $Fe(CO)_3$ fragment.

By extension, we suggest here that a related view may be employed to understand the bonding in **7b**, **8a**, and **8b**. If the HOMO electron density were fully localized on the phosphorus atom (e.g., in a P atom lone pair), oxidation by S or Se would be expected to produce a terminal thio- or selenophosphoryl species **7″**. Alternatively, a more ionic structure $^+P-E^-$ might develop in an intermediate species. The resulting electron-rich chalcogen could then donate into the M=P π^* LUMO orbital, resulting in formation of the $\overline{M-E-P}$ three-membered ring. This analysis, in fact, can be extended to rationalize the attack of carbenoid fragments observed by Malisch and our group on $Cp(CO)_2MP(X)(Y)$ species.

The unique result embodied by the structure of **7a** (long, terminal Mo−S bond) remains unrationalized by this picture. We can only suggest that small differences in relative orbital energies and characters for **4a** + S_8 (reactants) and the product **7a** must provide stabilization for this unexpected structure. It will be interesting to see if other reactions of **4a**,**b** and other examples of **2** produce related structural variations. These experimental results also may encourage higher level computational efforts on these interesting molecules.

Experimental Section

General Procedures. Standard inert-atmosphere techniques were used for the manipulation of all reagents and products. Infrared spectra were recorded on a Nicolet Model 6000 FT-IR spectrometer from NaCl solution cells or KBr pellets. Mass spectra were recorded from a Finnegan GC/MS system by using the solids inlet probe. NMR spectra were recorded from Varian FT-80A, GE NT-360, and JEOL GSX-400 NMR spectrometers. Spectral standards were Me_4Si (^1H

(17) The MO calculations related to **5** were performed on a simplified model containing a PH_2 fragment instead of the $P(Ph)[N(SiMe_3)_2]$ fragment.

and ^{13}C), H_3PO_4 (^{31}P), and Se (^{77}Se). $NaCpMo(CO)_3$,[18] $NaCpW(CO)_3$,[19] and $[(Me_3Si)_2N]P(Ph)Cl$[20] were prepared as described in the literature. All solvents were rigorously dried with appropriate drying agents, distilled, and stored over fresh drying agent.

Preparation of $Cp(CO)_2M\{P(Ph)[N(SiMe_3)_2]\}$ (M = Mo (4a), W (4b)). Typically, $[(Me_3Si)_2N]P(Ph)Cl$ (1.71g, 2.3 mmol) was injected dropwise over 10 min with a syringe through a septum port into a 100 mL Schlenk vessel held at −78 °C containing $NaCpM(CO)_3$ (2.3 mmol) dissolved in THF (50 mL) under dry nitrogen. During this time, the solution color changed from pale yellow to dark purple. The mixture was then warmed slowly to 23 °C and refluxed overnight under a nitrogen atmosphere. The solvent was vacuum evaporated from the resulting mixture, and the dark purple residue was extracted with benzene and filtered to remove solids (NaCl). The filtrate was evaporated to dryness leaving a purple microcrystalline solid. Yield: 90%. Multigram quantities of both reagents were obtained in an identical fashion by scaling up the starting quantities of reagents. The course of both reactions was also studied on a smaller scale for the purpose of measuring evolved CO with a Toepler pump. In each case, 90−100% of the expected 1 equiv of CO was recovered.

Oxidation Chemistry. Preparation of $Cp(CO)_2(S)M\{P(Ph)[N(SiMe_3)_2]\}$ (M = Mo, 7a), $Cp(CO)_2MSP(Ph)[N(SiMe_3)_2]$ (M = W, 7b), and $Cp(CO)_2MSeP(Ph)N(SiMe_3)_2$ (M = Mo (8a), W (8b)). In a typical reaction, **4a** (0.32 g, 0.67mmol) was dissolved in methylcyclohexane or benzene (50 mL) and cooled to −78 °C. To this stirred solution was added slowly a solution of sulfur (0.21 g, 0.67mmol) in methylcyclohexane or benzene (∼15 mL). Following addition, the mixture was warmed to 23 °C and stirred overnight. As the mixture approached room temperature, the dark purple solution turned yellow-orange. The resulting solution was filtered to remove a very small amount of suspended solid. The filtrate was evaporated to dryness leaving a microcrystalline solid, **7a**, which was recrystallized from either benzene or THF. Compounds **7b**, **8a**, and **8b** were prepared in an identical fashion. In each case, the product was a crystalline solid recovered in 95% or better yield following one recrystallization.

Characterization Data. 4a: purple solid; mp 155−157 °C. Anal. Calcd for $MoSi_2PO_2NC_{19}H_{28}$: C, 47.00; H, 5.81; N, 2.88. Found: C, 47.78; H, 5.99; N, 2.90. Mass spectrum (30 eV): *m/e* 487 (M^+, ^{98}Mo), 431 ($M - 2CO^+$, ^{98}Mo). Infrared spectrum (cyclohexane, cm^{-1}): 1948 (vs), 1876 (vs), 1256 (m), 1100 (w), 1081 (w), 1014 (m), 903 (m), 874 (m), 859 (m), 844 (m), 789 (w), 758 (w), 740 (w). $^{31}P\{^1H\}$ NMR (C_6D_6): δ 316. $^{13}C\{^1H\}$ NMR (CD_2Cl_2): δ 3.30 ($^3J_{CSiNP}$ = 2.7 Hz, *C*H_3), 93.13 ($^2J_{CMoP}$ = 1.7 Hz, *Cp*), 128−131 (complex multiplet, *Ph*). ^1H NMR (CD_2Cl_2): δ 0.32 (C*H*$_3$), 5.6 (*Cp*), 7.5 (*Ph*). **4b**: purple solid; mp 165−168 °C. Anal. Calcd for $WSi_2PO_2NC_{19}H_{28}$: C, 39.79; H, 4.92; N, 2.44. Found: C, 39.65; H, 5.02; N, 2.57. Mass spectrum (30 eV): *m/e* 575 (M^+, ^{186}W), 517 ($M - 2CO$, ^{186}W). Infrared spectrum (cyclohexane, cm^{-1}): 1941 (vs), 1869 (vs), 1255 (m), 1017 (w), 904 (m), 875 (m), 859 (m), 847 (m), 797 (w). $^{31}P\{^1H\}$ NMR (C_6D_6): δ 267, $^1J_{WP}$ = 702 Hz. $^{13}C\{^1H\}$ NMR (CD_2Cl_2): δ 3.28 ($^3J_{CSiNP}$ = 2.2 Hz, *C*H_3), 91.9 (*Cp*), 127−132 (complex multiplet, *Ph*). ^1H (CD_2Cl_2): δ 0.37 (C*H*$_3$), 5.73 (*Cp*), 7.53 (*Ph* complex multiplet). **7a**: orange solid; mp 147−150 °C. Anal. Calcd for $MoSPSi_2O_2NC_{19}H_{28}$: C, 44.09; H, 5.45; N, 2.71. Found: C, 44.74; H, 5.63; N, 2.84. Mass spectrum (30 eV): *m/e* 519 (M^+, ^{98}Mo), 491 ($M - CO^+$), 463 ($M - 2CO^+$). Infrared spectrum (cyclohexane, cm^{-1}): 1960 (vs), 1886 (vs). $^{31}P\{^1H\}$ NMR (CH_2Cl_2): δ 73. $^{13}C\{^1H\}$ NMR (CD_2Cl_2): δ 4.57 ($^3J_{CSiNP}$ = 3.9 Hz, CH_3), 4.94 (*C*H_3) 93.74 (*Cp*), 128−131 (multiplet, *Ph*). ^1H NMR (CD_2Cl_2): δ 1.45 (C*H*$_3$), 1.36 (C*H*$_3$), 5.51 (*Cp*), 7.37−7.45 (*Ph*). **7b**: orange solid; mp 212−214 °C. Anal. Calcd for $WSPSi_2O_2NC_{19}H_{28}$: C, 37.69; H, 4.66; N, 2.31. Found: C, 36.66; H, 4.73; N, 2.32. Mass spectrum (30 eV): *m/e* 606 (M^+, ^{186}W), 550 ($M - 2CO$). Infrared spectrum (cyclohexane, cm^{-1}): 1952 (vs), 1873 (vs). $^{31}P\{^1H\}$ NMR (C_6D_6): δ 33.9 ($^1J_{PW}$ = 268.6 Hz). $^{13}C\{^1H\}$ (C_6D_6): δ 4.43 (*C*H_3), 4.82 (*C*H_3), 91.8 (*Cp*), 128−139 (*Ph*). ^1H (C_6D_6): δ 0.54 (J_{PH} = 0.7 Hz, C*H*$_3$), 5.34 (Cp), 7.6−7.4 (Ph). **8a**: orange solid; mp 136−138 °C. Anal. Calcd for $MoSePSi_2O_2NC_{19}H_{28}$: C, 40.43; H, 5.00; N, 2.48. Found: C, 40.57; H, 5.27; N, 2.53. Mass spectrum (30 eV): *m/e* 567 (M^+, ^{98}Mo, ^{80}Se), 539 ($M - CO^+$), 511 ($M - 2CO^+$), 431 ($M - Se^+$). Infrared spectrum (cyclohexane, cm^{-1}): 1959 (vs), 1886 (vs). $^{31}P\{^1H\}$ NMR (C_6D_6): δ 85.9 (J_{PSe} = 497.8 Hz). $^{13}C\{^1H\}$ (C_6D_6): δ 4.77 (J_{PC} = 2.7 Hz, *C*H_3), 92.9 (*Cp*), 128.9−142. (Ph) ^1H NMR (C_6D_6): δ 0.5 (J_{PH} = 2.2 Hz; C*H*$_3$), 5.24 (Cp), 7.8 (Ph). **8b**: orange solid; mp 136−138 °C. Anal. Calcd for $WSePSi_2O_2NC_{19}H_{28}$: C, 34.98; H, 4.33; N, 2.15. Found: C, 34.88; H, 4.48; N, 2.15. Mass spectrum (30 eV): 653 (M^+, ^{184}W, ^{80}Se), 597 ($M - 2CO^+$). Infrared spectrum (cyclohexane, cm^{-1}): 1951 (vs), 1875 (vs). $^{31}P\{^1H\}$ NMR (C_6D_6): δ 43.9 (J_{PW} = 290.2 Hz, J_{PSe} = 469.2 Hz). $^{13}C\{^1H\}$ (C_6D_6): δ 4.56 (*C*H_3), 4.98 (J_{PC} = 3.0 Hz, *C*H_3), 91.29 (Cp), 128−140 (Ph). ^1H (C_6D_6): δ 0.27 (J_{PH} = 2.5 Hz, C*H*$_3$), 5.06 (Cp), 7.4 (Ph).

Crystal Structure Determinations. Single crystals of **4a**, **7a**,**b**, and **8a** were obtained by cooling saturated solutions of the compounds to −20 °C and allowing these to stand for 1−14 days at −10 °C. Crystals were sealed in glass capillary tubes under dry nitrogen. Data were collected on a Siemens P3/F four circle diffractometer using Mo Kα (λ = 0.710 69 Å) at 20 °C radiation, a scintillation counter, highly oriented graphite crystal monochromator, and pulse height analyzer. An empirical absorption correction based upon ψ scans was applied to each data set. Redundant and equivalent data were averaged and converted to unscaled $|F_o|$ values following corrections for Lorentz and polarization effects. The calculations were performed on a Siemens P3 structure solution system using SHELXTL programs. Neutral atom scattering factors were employed. The structures were solved by standard heavy atom methods. Non-hydrogen atoms were refined anisotropically and hydrogen atoms isotropically with $U_{iso} = 1.2U_{eq}$ for the parent atom. A summary of crystallographic data are presented in Table 1.

Acknowledgment is made to the National Science Foundation Grant CHE-8503550 for support of this research. We also wish to thank our colleague, Professor J. V. Ortiz, for stimulating discussion over the bonding in these compounds.

Supporting Information Available: Tables of data collection and structure solution details, fractional atomic coordinates and *U* values, anisotropic displacement factors, full bond distances and angles, and H coordinates for **4a**, **7a**,**b**, and **8a** (41 pages). Ordering information is given on any current masthead page.

OM9605490

(18) King, R. B.; Iqbal, M. Z.; King, A. D. *J. Organomet. Chem.* **1979**, *171*, 53.
(19) Fischer, E. O. *Inorg. Synth.* **1963**, *7*, 136.
(20) McNamara, W. F.; Reisacher, H.-U.; Duesler, E. N.; Paine, R. T. *Organometallics* **1988**, *7*, 1313.